Composites Science and Technology xxx (2009) xxx–xxx

Contents lists available at ScienceDirect

Composites Science and Technology

journal homepage: www.elsevier.com/locate/compscitech

Effect of hygrothermal ageing on morphology and indentation modulus of injection moulded nylon 6/organoclay nanocomposites

Rocio Seltzer [a], Patricia M. Frontini [b], Yiu-Wing Mai [a,*]

[a] Center for Advanced Materials Technology (CAMT), School of Aerospace, Mechanical and Mechatronic Engineering J07, University of Sydney, Sydney, Australia
[b] Instituto de Investigaciones en Ciencia y Tecnología de Materiales (INTEMA), Departamento de Materiales, Universidad de Mar del Plata, Mar del Plata, Argentina

ARTICLE INFO

Article history:
Received 23 October 2008
Received in revised form 21 January 2009
Accepted 22 January 2009
Available online xxxx

Keywords:
A. Nanocomposites
B. Hygrothermal effect
B. Mechanical properties
E. Injection moulding

ABSTRACT

The effect of water immersion on the morphology and indentation modulus of injection moulded nylon 6 and its organoclay nanocomposites was investigated. XRD analysis showed that at 70 °C water promoted further crystallization in the nylon matrix and aided the γ- to α-crystal phase transition in the skin region. However, the presence of organoclay deterred this transformation. The combined actions of water and heat (70 °C) did not further degrade nylon 6 and its nanocomposites compared to water ageing at room temperature (25 °C). In fact, there was relative enhancement of the indentation moduli owing to the beneficial morphological changes induced in the nylon matrix. The largest improvements were found in the skin region of the injection moulded bars.

1. Introduction

Nylon 6 is widely used in automotive applications due to its superior mechanical properties, tribological performance and chemical resistance. However, immediately after moulding, nylon products are extremely dry making them rather brittle. Nylons are highly hygroscopic, and eventually take up moisture, which increases their toughness. The rate of moisture absorption in humid air at room temperature is slow and it may take several weeks to reach equilibrium depending on the dimensions of the part concerned. To accelerate this process, nylon products are often preconditioned by submersion in water at temperatures between 50 °C and 100 °C.

Unfortunately, hygrothermal ageing, as this treatment is generally called, is known to provoke chemical and physical changes in nylon 6, such as hydrolysis of the polymer bonds and micro-void formation, respectively [1,2]. In nylon-based fibre composites, fibre/matrix interface degradation may occur [2,3]. Consequently, different moisture conditioning treatments lead to different final mechanical properties.

Nano-particles have shown to confer polymers better mechanical properties than micro-particles [4–6] due to their high surface area and stiffness. Nano-particles are also expected to have remarkable impact on hygrothermally aged materials. However, depending on the matrix/particle system, nano-particles may have different effects on water sorption and ultimate mechanical properties of the polymers. Chow et al. [7] discovered that polystyrene absorbs more water when organoclay is added due to its hydrophilicity. Since the particle/matrix interface is debilitated, the addition of organoclay is also detrimental for the impact properties of the hygrothermally aged polystyrene. In contrast, however, when organoclay is added to polyamide 6/polypropyelene blend, Chow et al. [8] found that the retention ability and recovery properties are increased. Organoclay [9] and graphitic nano-fibres [10] are also shown to enhance the resistance to hygrothermal ageing of epoxy.

The effect of moisture on nylon 6/organoclay nanocomposites has already been studied [11,12], but water conditioning was performed at 70 °C in all cases to increase the rate of water uptake. To discern the individual effects of water and heat, it is necessary to condition the samples also at low temperatures. Unfortunately, water conditioning at room temperature may take up to several months depending on the thickness of the sample. Hence, one effective way to overcome this difficulty is to test very small specimens. Nanoindentation is an emerging technique which has been widely used to determine the mechanical properties of small components [13,14]. In the present investigation, this type of mechanical test not only saved time in regard to water conditioning of the samples, but it also enabled the study of the effect of hygrothermal ageing in different regions of the injection moulded specimens.

It is well-known that many polymers and polymer composites possess markedly different morphology in the skin and core regions. Thus, the interaction with water and heat will have different consequences in each region. In particular, injection moulded nylon 6/organoclay nanocomposites exhibit higher crystallinity and

* Corresponding author. Tel.: +61 2 9351 2290; fax: +61 2 9351 3760.
E-mail address: y.mai@usyd.edu.au (Y.-W. Mai).

0266-3538/$ - see front matter © 2009 Elsevier Ltd. All rights reserved.
doi:10.1016/j.compscitech.2009.01.029

γ- to α-crystals ratio in the surface than in the core [15]. Moreover, the clay particles are unevenly distributed in the specimen, the concentration being higher in the core than in the surface [16,17]. Furthermore, it has been observed that in injection moulded nylon 66/organoclay nanocomposites the clay platelets located near the surface are aligned parallel to the wall of the mould, while the platelets in the core are randomly rotated about the injection-moulding direction [16–18].

This work aims to elucidate the morphological changes induced by hygrothermal ageing in both the skin and core regions of injection moulded nylon 6/organoclay nanocomposites and to study the effects of those changes on the elastic modulus via nano-indentation tests.

2. Experimental work

2.1. Materials

Nylon 6 (Akulon F 232-D) was obtained from DSM Engineering Plastics and the organoclay used was Cloisite® 30B supplied by Southern Clay Products Inc. via Jim Chambers & Associates, Australia. It was organically modified with alkyl ammonium surfactant, namely methyl, tallow, bis-2-hydroxyethyl quartenary ammonium chloride, having a cation exchange capacity of 90 mequiv/100 g. All the samples were dried in a vacuum oven at 80 °C for 24 h before melt blending. A wide range of nylon 6/organoclay nanocomposites containing 0, 2.5, 5, 7.5, and 10 wt% organoclay (denoted by N0.0, N2.5, N5.0, N7.5 and N10.0, respectively) were prepared by melt compounding using a ZSK 30 twin-screw extruder and then injection moulded to dumb-bells and rectangular bars for mechanical testing.

2.2. X-ray diffraction

X-ray diffraction patterns were obtained using a Siemens D5000 X-ray diffractometer with CuKα radiation (λ = 1.5405 Å) at a generator voltage of 40 kV and a current of 30 mA. All experiments were conducted in the reflection mode at ambient temperature with 2θ varying between 1° and 30° at a speed of 1°/min and a step size of 0.05°. To study the effect of hygrothermal ageing on nylon 6 and its nanocomposites, three sets of samples were tested: as-moulded bars, bars dried in oven at 80 °C for 24 h, and bars immersed in water at 70 °C for 3 weeks to reach saturation. Scans were conducted on the surfaces and mid-thickness along the flow direction of these injection moulded bars. To study the mid-thickness, the bars were cut after being pre-conditioned.

From the XRD traces, after de-convoluting the curves to crystalline and amorphous peaks, the crystallinity was calculated as the ratio between the areas under the crystalline peaks and the amorphous halo. The percentage of the α-phase with respect to the γ-phase was calculated by:

$$\alpha(\%) = \frac{A_\alpha}{A_\alpha + A_\gamma} \tag{1}$$

where A_α is the area under the two α-peaks and A_γ is the area under the γ-peak.

2.3. Differential scanning calorimetry

Thermal tests were conducted on slices cut from cross-sections of injection moulded bars by using a Perkin Elmer thermal analyser DSC-7. The samples were heated at a scanning rate of 5 °C min^{-1} under a nitrogen atmosphere in order to reduce the risk of oxidation.

The crystallinity (X_C) of injection moulded samples was calculated from the enthalpy evolved during crystallization based on the cooling scans by:

$$X_C = \frac{\Delta H_C}{(1-\phi)\Delta H_m^0} \times 100 \tag{2}$$

where ΔH_C is apparent enthalpy of crystallization of sample, ΔH_m^0 is extrapolated enthalpy value corresponding to melting of 100% crystalline pure nylon 6, which is taken as 230 J/g [19], and φ is weight fraction of MMT in the nanocomposites.

2.4. Transmission electron microscopy

Cross-sectional transmission electron microscopy (TEM) images were taken perpendicular to the injection flow direction of as-moulded samples. Ultra-thin sections between 60 and 90 nm in thickness were cryogenically cut with a diamond knife in a liquid nitrogen environment by using a Reichert-Jung Ultracut E microtome. Sections were collected on 300-mesh copper TEM grids and then dried with filter paper. Examination of the specimens was conducted on a Hitachi-800 TEM at an accelerating voltage of 22 kV.

2.5. Tensile tests

Young's moduli of both dried and water-saturated samples were determined by tensile tests using an Instron 5567 testing machine. Drying was performed in an oven at 80 °C for 24 h, while water saturation was reached by immersion in water at 70 °C for 3 weeks as described before. Until testing, the dried samples were kept in a desiccator, while the water-saturated samples were kept in water. The tests were conducted on injection moulded dumbbell specimens at a crosshead speed of 5 mm/min. An extensometer was used to measure the elongation within a gauge length of 50 mm. All these tests were conducted at ambient temperature (20–25 °C) and an average value of five repeated tests was taken for each composition.

2.6. Nano-indentation

The mechanical responses in the surface (skin) and mid-thickness (core) regions of injection moulded bars, (see Fig. 1), were determined by depth sensing indentation with nano-scale resolution. Indentation measurements were performed using a fully calibrated UMIS nano-indenter from CSIRO, Australia, details of which are published elsewhere [20]. Its potential for highly accurate measurements is illustrated by the parameters: displacement resolution 0.1 nm, internal noise uncertainty <0.1 nm, force resolution 0.75 μN and stage registration repeatability 0.2 μm. Load, P, and depth, h, were recorded simultaneously for a complete load-hold-unload cycle using a spherical indenter with a radius, R, of 20 μm. The contact force for detection of the surface position was 0.05 mN and the loading rate was 10 mN/s.

To obtain smooth surfaces, ~2 μm were removed from the indentation specimens by using a microtome. The samples were pre-conditioned in three different ways: drying in an oven at 80 °C for 24 h and immersion in water at 25 °C and 70 °C to satura-

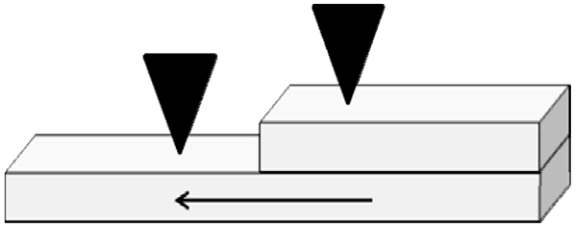

Fig. 1. Schematic of an indentation moulded bar showing the two indentation locations (the arrow shows the injection flow direction).

tion. The dried samples were tested within 2–4 h after removal from the oven. The tests on water-conditioned samples were performed immersed in water to ensure moisture equilibrium at all times. Ten indentations separated by a distance 100 μm were made on each sample. The elastic modulus [21], E, was calculated from:

$$E = \frac{\pi}{2(1-\nu^2)}\frac{S}{\sqrt{a}} \tag{3}$$

$$S = \left.\frac{dP_u}{dh}\right|_{h\,\max} \tag{4}$$

where ν is the Poisson's ratio, a is the contact area corresponding to the maximum load $P_{\max}$, S is the stiffness at the onset of unloading, and h is the indentation depth.

In the case of a relatively small indentation depth, a spherical indenter can be approximated as a paraboloid of revolution. Then, the contact depth, h_c, is given by:

$$h_c = h_{\max} - 0.75\frac{P_{\max}}{S} \tag{5}$$

From geometric considerations, the contact area is:

$$a = \pi h_c(2R - h_c) \tag{6}$$

The stiffness at onset of unloading, S, used in the calculations is affected by the viscoelastic behaviour displayed by the tested material. If it is creeping under the load of the indenter tip which is suddenly reduced, as in a triangular load pattern, the displacement may continue to increase even after reducing the applied load. This behaviour creates an abrupt slope change in the unloading curve as the material begins to recover, making it difficult to determine the unloading slope. Ngan and Tang [22] proposed that, in such a viscoelastic situation, the correct elastic stiffness S_e to be used in Eqs. (3) and (7) in place of S can be obtained from:

$$\frac{1}{S_e} = \frac{1}{S} + \frac{\dot{h}_h}{\dot{P}_u} \tag{7}$$

where $\dot{h}_h$ is the indenter-tip displacement rate at the end of the load-hold period just prior to unload, and $\dot{P}_u$ is the unloading rate.

3. Results and discussion

3.1. Organoclay dispersion

From the XRD pattern shown in Figs. 2 and 3, it is clear that only in the nanocomposite with the least clay content are the particles not fully exfoliated, neither in the core nor in the skin regions, given the organoclay used, Cloisite® 30B, has a d-spacing equal to 1.8 nm and corresponding to $2\theta = 4.9°$, and there is a basal diffraction peak in the range of $2\theta = 3–5.5°$. In Fig. 3, the XRD curves of nylon 6 nanocomposites with 5 wt% clay and above display a broad peak in the range of $2\theta = 1.5–6°$, which has been attributed to extensive orientation of clay platelets parallel to the walls of the mould during injection moulding [17,18]. Fig. 4 shows TEM images of the mid-sections (core) of the nylon nanocomposites. Consistent with the XRD results, the dispersion of the organoclay is improved with increasing loading. Clusters of stacked sheets are clearly shown in the nanocomposite with 2.5 wt% organoclay. Conversely, in nylon with more than 5 wt% organoclay, the clay is mostly exfoliated. The best dispersion seems to be that obtained with 10 wt% organoclay. It is noted that complete exfoliation has been achieved in similar systems even at an organoclay loading of 2.5 wt% [12]. This is because the degree of clay dispersion not only depends on the affinity and compatibility of organoclay with the matrix (which is an intrinsic factor dependent on the materials), but also on the shear stress (which is an extrinsic factor dependent on processing conditions and clay loading) [23–25]. Hence, the fact that, in our case, organoclay exfoliation is not complete at the lowest clay loading is because the imposed processing conditions do not generate a shear force in the mix strong enough to delaminate completely the clay agglomerates. The improved dispersion at higher clay loadings is most probably due to the increased initial viscosity, which, consequently, increases the shear force among the platelets [26].

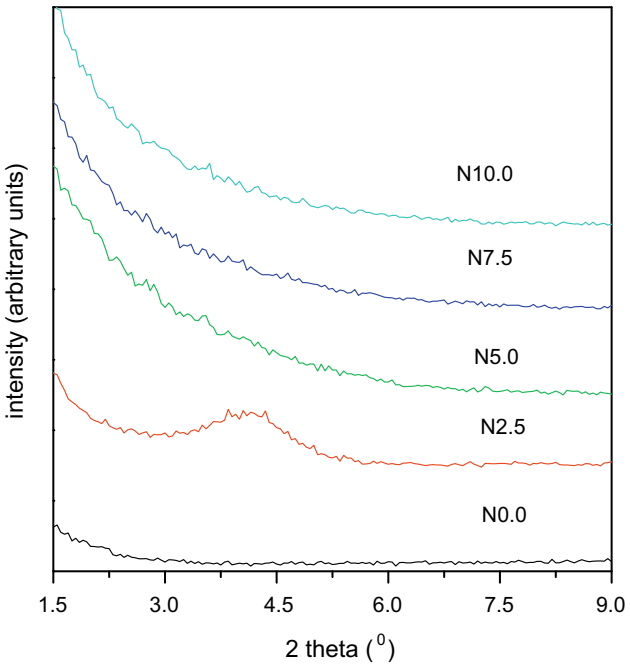

Fig. 2. XRD patterns of nylon 6 and its nanocomposites in the range of clay d-spacing measured on cross-sections transverse to the injection flow direction (core region).

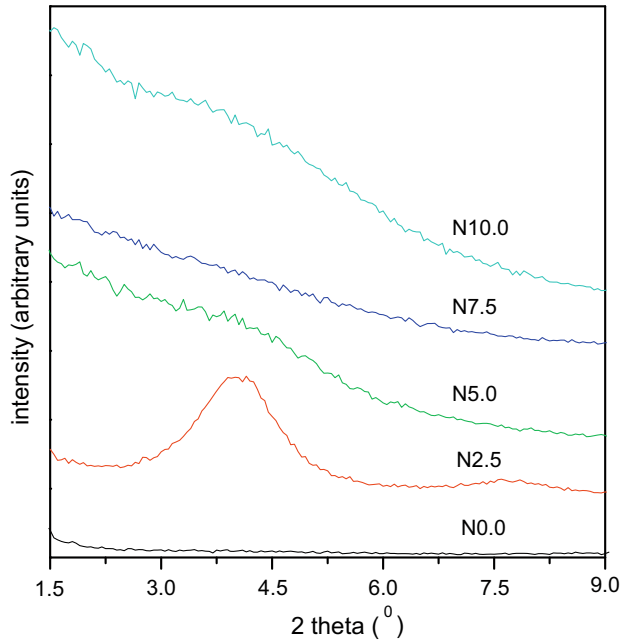

Fig. 3. XRD patterns of as-moulded samples of nylon 6 and its nanocomposites in the range of clay d-spacing measured on the surface parallel to the injection flow direction (skin region).

Please cite this article in press as: Seltzer R et al. Effect of hygrothermal ageing on morphology and indentation modulus of injection ... Compos Sci Technol (2009), doi:10.1016/j.compscitech.2009.01.029

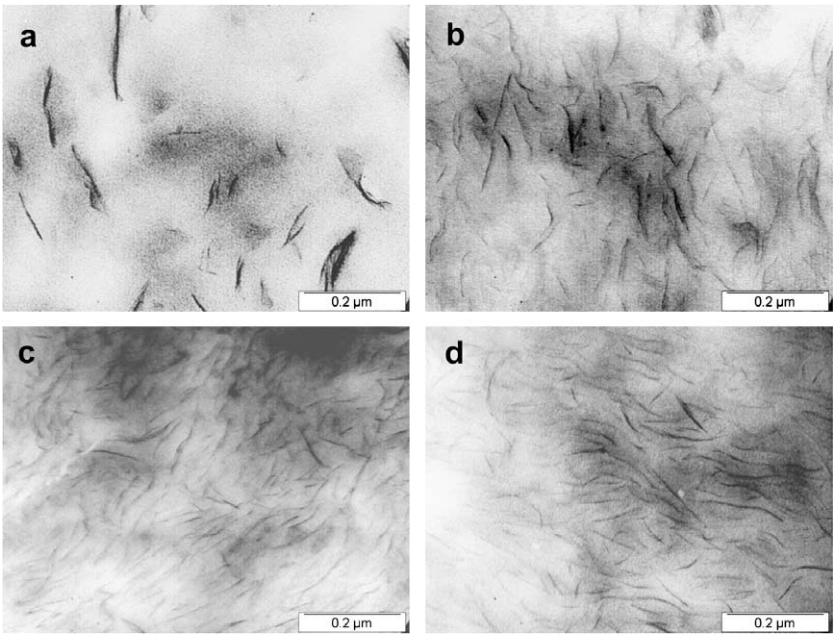

Fig. 4. TEM images of as-moulded samples showing clay dispersion in the core regions of (a) N2.5, (b) N5.0, (c) N7.5 and (d) N10.0.

3.2. Effect of hygrothermal ageing on crystal morphology

Injection moulded specimens of nylon 6 are known to have a skin-core structure (e.g., Murthy et al. [27]). To compare the morphology of both regions, the bar surface and mid-section crystal morphologies were studied by XRD. Fig. 5 shows the XRD patterns of as-moulded nylon 6 and its nanocomposites where scanning was conducted on mid-sections of the moulded bars parallel to the injection flow direction. The peaks at $2\theta \approx 20.2°$ ($\alpha 1$) and 23.4° ($\alpha 2$) are assigned to (200) and (202) + (002) planes of nylon 6 α-crystals, respectively; while the peak at $2\theta \approx 21.3°$ is assigned to (200) + (001) plane of γ-form [28]. According to the XRD patterns displayed in Fig. 5, the α-form is predominant in the core region of all as-moulded samples, while the high temperature γ-form is only stabilized when organoclay is added, which is in agreement with many other works [5,15–18,23,29,30]. It has been suggested that clay platelets have a similar effect as quenching, that is, they limit chain mobility [30]. The α-crystals are thermodynamically stable at room temperature, while the γ-crystals are more stearically favourable. Hence, when the mobility of nylon 6 molecules is somehow restricted, the γ-form is favoured over the α-form.

The X-ray patterns of the skin regions of the as-moulded materials are shown in Fig. 6. Neat nylon 6 has a peak at $2\theta \approx 21.2°$, corresponding to the γ-crystals and a milder peak at $2\theta \approx 23.1°$, corresponding to the α-crystals. The presence of γ-crystals is the

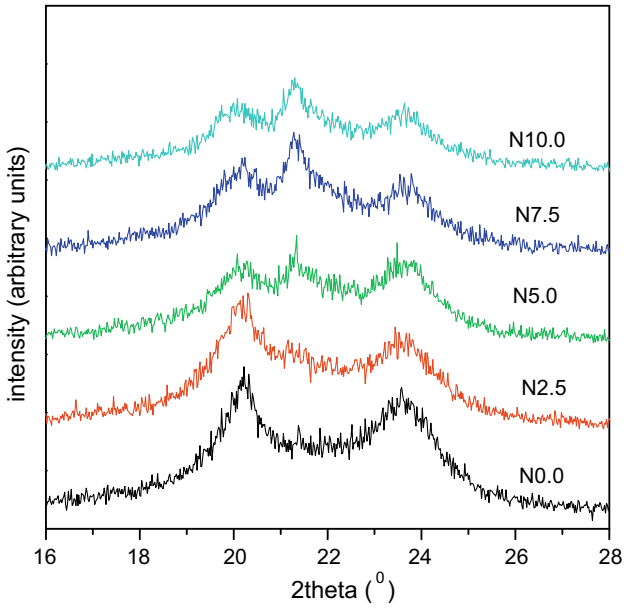

Fig. 5. XRD patterns of the core regions of as-moulded injection moulded nylon 6 and its nanocomposites.

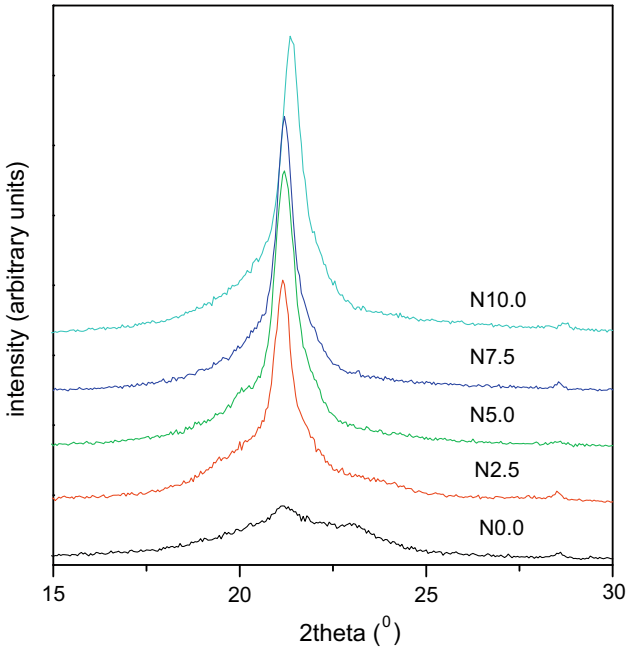

Fig. 6. XRD patterns of the skin regions of as-moulded injection moulded nylon 6 and its nanocomposites.

major difference between the skin and core morphologies. This occurs because of the cooling rate gradient such that it is faster in the outer layers and slower towards the centre of the specimen. It is known that the γ-form crystals are observed on quenching from the melt, while the α-form results from slow cooling of the melt [31]. The presence of organoclay has a similar effect as quenching, since it hinders molecular mobility.

XRD scans were also performed on the pre-conditioned samples at high temperature, that is, dried or annealed at 80 °C for 24 h, and immersed in water at 70 °C for 3 weeks. The XRD patterns of the skin and core regions of the annealed samples (not shown here) remained unchanged compared to as-moulded samples, meaning there was no modification of the crystal structure or crystallinity. Although the XRD patterns of the core of hygrothermally aged samples were similar to the as-moulded samples, the XRD scans of the skin showed quite different curve shapes. These results are shown in Fig. 7. α_1-peaks at $2\theta \approx 20.5°$ appear in all samples, while α_2-peaks at $2\theta \approx 23.5°$ are also seen in neat nylon and its nanocomposite with 2.5 wt% clay. These new peaks confirm a phase transformation. Indeed, phase transition from γ- to α-crystals in dry neat nylon 6 and nanocomposites has been reported to occur upon annealing over 120 °C [32]. In the presence of moisture, the chains in the meta-stable γ-phase are sufficiently mobile to assume the more stable, lower energy conformation, hence partially converting them to the α-form. According to our ageing experiments in water, as evidenced in Fig. 7, this crystal phase transformation happens at a temperature of 70 °C. However, at 25 °C, no such phase transformation occurs in water.

The percentage of the α-phase with respect to the total crystalline phase consisting of α- and γ-crystals in nylon 6 and its nanocomposites is shown in Fig. 8. Neat nylon gives only α-crystals in the core. When organoclay is added, the high temperature γ-crystals are stabilized, and its proportion increases with organoclay loading. In the skin, the γ-phase predominates in all samples including neat nylon, comprising ~70% of the crystalline phases.

As mentioned above, during hygrothermal ageing at 70 °C, there is a phase transformation in the skin, while the crystal morphology

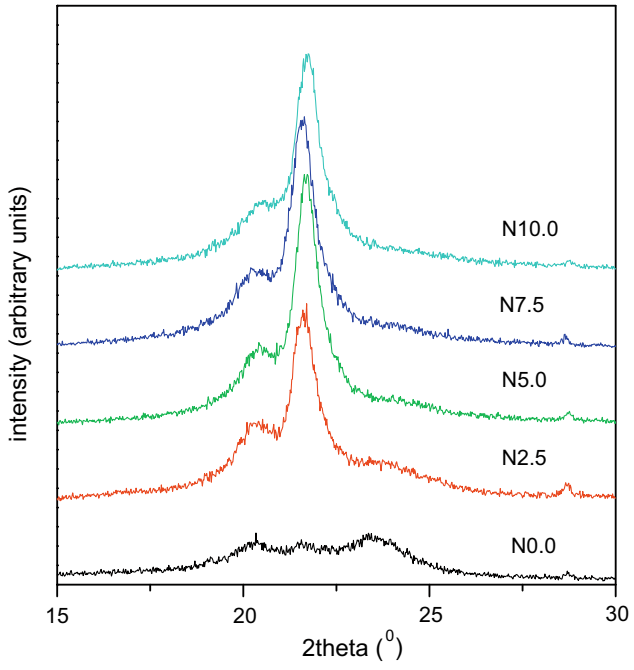

Fig. 7. XRD patterns of the skin regions of hygrothermally aged nylon 6 and its nanocomposites.

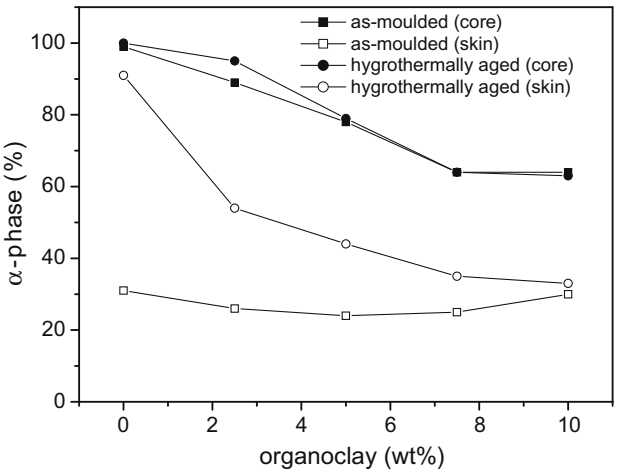

Fig. 8. α-crystal percentage of nylon 6 as a function of organoclay content calculated from XRD scans.

of the core remains unchanged. In neat nylon, most γ-crystals are transformed into α-form, resembling the structure of the core. Nanocomposites also undergo a γ to α transformation, but it is milder and decreases with organoclay loading. This supports the statement that clay platelets stabilize the γ-phase in nylon 6.

3.3. Effect of hygrothermal ageing on crystallinity

The most widely used techniques to determine crystallinity of thermoplastics are XRD and DSC. Since both have shortcomings, they are often used conjointly to complement each other [28]. The crystallinity calculated from the XRD scans as a function of organoclay loading is shown in Fig. 9a. It seems that organoclay increases the crystallinity in the skin region, but not in the core. However, Kojima et al. [33] have shown that organoclay induces crystallites orientation parallel to the mould walls in the near surface of injection moulded nylon 6, which exaggerates the intensity of the crystalline XRD peaks. Conversely, in the core there are no such artefacts since the crystals are randomly oriented. Despite this distortion in the XRD data in the skin region, there are two definitive conclusions that can be confidently extracted. These are, the crystallinity of the core is unaltered by the presence of organoclay, and hygrothermal ageing increases slightly the crystallinity of the samples except at the highest organoclay loading.

The crystallinity determined from DSC thermograms is shown in Fig. 9b. The values for the core region are close to those obtained from XRD, but the values in the skin differ considerably. As already discussed, the crystallinity measured with XRD in the skin region of the nanocomposites is overestimated due to the preferred orientation of the crystallites. Even though the interpretation of the DSC data is also prone to errors, the source of these errors is the same for skin and core so that their values can be compared. Hence, it can be affirmed that the crystallinities in the skin and core regions are similar. However, the subtle effect of hygrothermal ageing on crystallinity cannot be seen from the results in Fig. 9b but can only be obtained from the XRD results in Fig. 9a. That is, the crystallinity of all the samples increases slightly with hygrothermal ageing (except at 10 wt% clay).

3.4. Nano-indentation modulus

As shown in Table 1, when nylon 6 and its nanocomposites are saturated with water, the indentation modulus decreases between one-half and one-third compared to the dry values. This contrasts with the results of bulk tests where the reduction is between one-

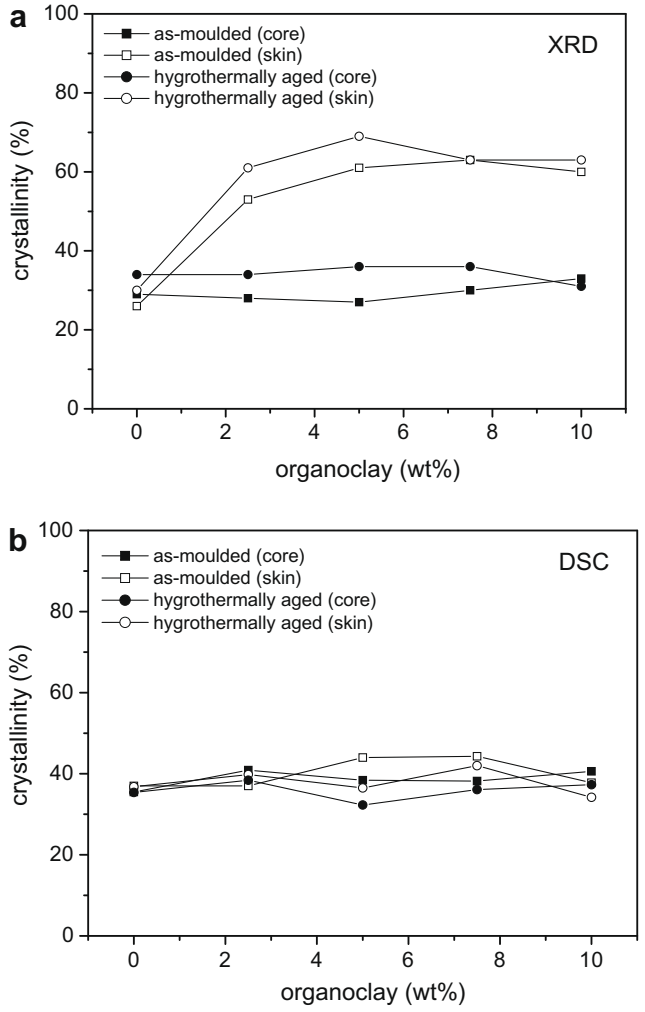

Fig. 9. Crystallinity of nylon 6 as a function of organoclay content calculated from. (a) XRD scans and (b) DSC heating curves.

fifth and one-sixth of the dry moduli [1]. In the following section, it will be shown why the results obtained for the dry samples are not *true* values.

By analysing the results of the water-conditioned samples at 25 °C, it is noted that the skin and core elastic moduli of neat nylon 6 are similar. However, for the nanocomposites, the skin is between 20% and 55% stiffer than the core. This difference can be explained in terms of the crystal morphology and crystal orientation as shown schematically in Fig. 10. All the samples have greater proportion of α-phase in the core than in the skin region. This should result in a stiffer core, since it is known that the α-crystals have a higher modulus than the γ-crystals [34–36]. However, the soft γ-crystals in the skin are counteracted by molecular orientation in the neat nylon, and by molecular, organoclay and crystal orientation in the nanocomposites. In the case of neat nylon, both effects are balanced out, while in the nanocomposites the orientation plays a predominant role resulting in a skin with better mechanical properties than the core region. Although the orientation referred to here is perpendicular to the applied load, it affects the indentation modulus [37].

Hygrothermal ageing at 70 °C, unlike hygrothermal ageing at 25 °C, induces changes in the crystalline structure of the nylon matrix. Apparently, there is a small increment in the crystallinity as detected with XRD, but the major change is the transformation of γ-phase to α-phase in the outermost layers. Both changes are translated into stiffening of the skin region relative to hygrothermally aged samples at 25 °C, as seen in Table 1. This relative enhancement in indentation moduli is the most noticeable in neat nylon 6, since the organoclay mitigates the γ–α transition. Given the absence of morphological changes in the inner layers, the mild relative improvement of the core properties can only be attributed to the slight increment in crystallinity. The fact that the core moduli of samples hygrothermally aged at 70 °C are not lower than the core moduli of samples hygrothermally aged at 25 °C is an important result because it indicates that water at high temperature (up to 70 °C) does not further degrade nylon 6 or its nanocomposites.

3.5. Relationship between macro and nano-mechanical response

Macro-mechanical tests, such as tensile testing, are a reflection of the average response of a specimen, while nano-indentation is capable of capturing the local mechanical behaviour. The gap separating these two types of tests is not only one of scale. Mechanical properties determined from tensile and indentation data may differ due to dissimilar induced stress states and differences in the orientation of the applied load, among others. In this section, the relationship between local and average mechanical response as measured by tensile and indentation tests is discussed.

Nylon 6 and its organoclay nanocomposites have already been studied by nano-indentation and the results between tensile and indentation properties have also been compared [36–38]. In all cases, it was found that the indentation moduli are considerably lower than the tensile moduli. The difference between indentation (Table 1) and tensile (Table 2) moduli measured in our laboratory are similar to the ones found in the aforementioned publications [38–40]. To explain these results, indentation tests on dried samples were repeated after exposing them to normal ambient humidity for 7 days. The moduli obtained were only 10% lower indicating that in the first few hours in contact with humid air the skin almost reached moisture equilibrium. That is, the dried samples inevitably absorb ambient moisture from the skin before being tested. Therefore, the indentation (skin) moduli are lower than the tensile (bulk) moduli as reported here and in [38–40]. However, this also means that extreme care has to be taken to measure *true* dry nano-indentation properties for nylon 6 and its nanocomposites.

By inspecting the tensile and indentation results of the samples hygrothermally aged at 70 °C, it is evident that the skin and tensile moduli are similar, while the core moduli are lower. To analyse this fact it must be taken into account that the relationship between tensile and indentation moduli is a complex one due to the inho-

Table 1
Elastic moduli determined from indentation tests of nylon 6 and its nanocomposites after drying (D) and hygrothermal ageing at 25 °C (HA-25) and 70 °C (HA-70).

Material	E_D (GPa)	Skin region			Core region	
		E_{HA-25} (GPa)	E_{HA-70} (GPa)	E_D (GPa)	E_{HA-25} (GPa)	E_{HA-70} (GPa)
N0.0	1.02 ± 0.01	0.45 ± 0.01	0.68 ± 0.03	1.27 ± 0.02	0.46 ± 0.01	0.48 ± 0.02
N2.5	1.57 ± 0.01	0.75 ± 0.03	0.94 ± 0.03	1.55 ± 0.07	0.61 ± 0.02	0.68 ± 0.01
N5.0	1.99 ± 0.02	0.91 ± 0.05	1.13 ± 0.05	1.81 ± 0.06	0.66 ± 0.01	0.79 ± 0.01
N7.5	2.09 ± 0.05	0.98 ± 0.06	1.16 ± 0.01	2.11 ± 0.08	0.80 ± 0.04	0.87 ± 0.01
N10.0	2.22 ± 0.05	1.1 ± 0.06	1.12 ± 0.05	2.21 ± 0.12	0.70 ± 0.032	0.73 ± 0.01

Please cite this article in press as: Seltzer R et al. Effect of hygrothermal ageing on morphology and indentation modulus of injection ... Compos Sci Technol (2009), doi:10.1016/j.compscitech.2009.01.029

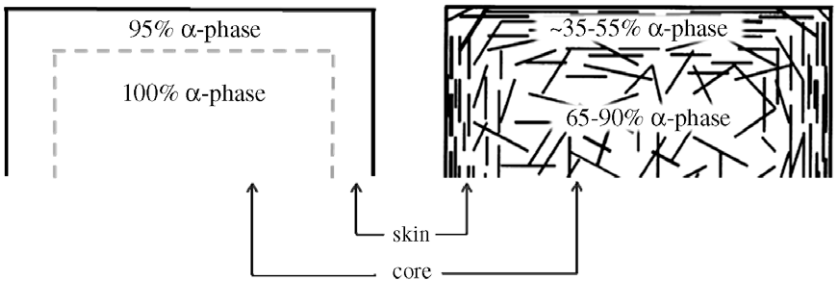

Fig. 10. Diagram showing the morphology in neat nylon (left) and clay orientation in the nylon 6 nanocomposites (right) injection moulded specimens hygrothermally aged at 25 °C.

Table 2
Elastic moduli determined from tensile tests of bulk nylon 6 and its nanocomposites after drying (D) and hygrothermal ageing at 70 °C (HA-70).

Material	E_D (GPa)	E_{HA-70} (GPa)
N0.0	2.51 ± 0.03	0.67 ± 0.07
N2.5	2.72 ± 0.11	0.77 ± 0.04
N5.0	3.28 ± 0.06	0.97 ± 0.06
N7.5	3.72 ± 0.04	1.19 ± 0.06
N10.0	3.90 ± 0.13	1.33 ± 0.02

mogeneity and anisotropy of the materials. The skin and core mechanical response is individually identified by indentation, while the moduli obtained in tensile tests are an average of these two regions. The problem of analysing the indentation modulus is that the stress field generated by indentation is three-dimensional. As a consequence, the measured modulus lies somewhere between E_{11}, E_{33} and E_{22} (conventions for the directions are shown in Fig. 11) [37]. We know that: $E_{skin} = f\ (E_{11\_skin}, E_{22\_skin}, E_{33\_skin})$, $E_{core} = f\ (E_{11\_core}, E_{22\_core}, E_{33\_core})$, and $E_{tensile} = f\ (E_{11\_skin}, E_{11\_core})$. Thus, the fact that the tensile and skin elastic moduli are similar in most hygrothermally aged samples at 70 °C is just a coincidence.

Another issue that deserves discussion is the degree of stiffening conferred by the organoclay as measured in indentation and tension tests. Fig. 12 shows the moduli of the nanocomposites normalized to neat nylon 6 modulus and plotted as a function of organoclay loading. The tensile modulus is often taken as an indicator of clay exfoliation [41]. As seen in Section 3.1, the organoclay is mostly intercalated when its loading is 2.5 wt% and mostly exfoliated above this percentage, which is reflected in a low initial increment of the tensile modulus followed by a steep increase. On the contrary, the modulus measured in indentation seems to be insensitive to the degree of exfoliation of clay. The initial steep increment is most likely due to the local increase in particle concentration directly underneath the indenter tip when it is pushed into the specimen, as demonstrated by Shen and Guo [42] using finite element analysis. However, the decreasing rate of stiffness

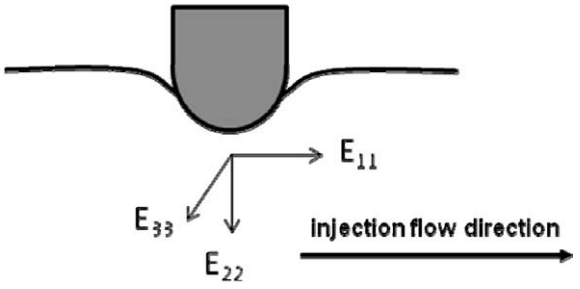

Fig. 11. Scheme showing the convention of axis orientation with respect to the indentation load and injection flow.

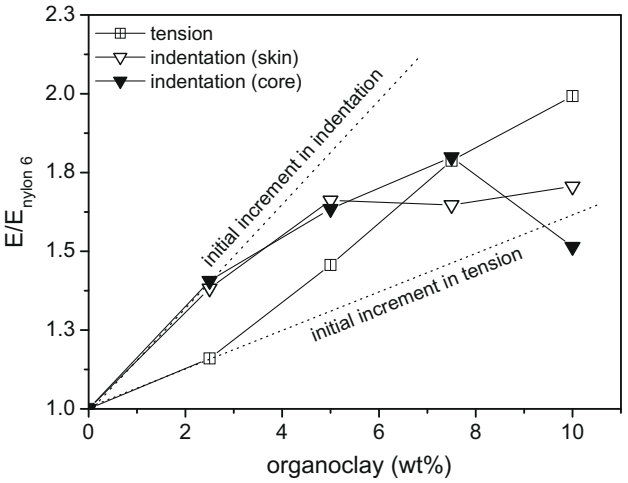

Fig. 12. Normalized moduli as a function of organoclay content of samples hygrothermally aged at 70 °C.

enhancement with organoclay content is more difficult to explain due to the increasingly complex morphologies under the indenter.

4. Conclusions

(a) Hygrothermal ageing reduces the elastic moduli of nylon 6 and its organoclay nanocomposites relative to their respective dry materials. However, it is shown that hygrothermal ageing at 70 °C does not cause further degradation in the elastic moduli compared to ageing in water at 25 °C, neither in the neat polymer, nor in its nanocomposites.

(b) Hygrothermal ageing at 70 °C induces structural modifications to nylon 6, such as increments in crystallinity and transformation of γ- to α-crystals. Because organoclay tends to stabilize the γ-form, the γ–α crystal transition is partially inhibited in the nylon/organoclay nanocomposites. Hence, the improvements in elastic moduli due to hygrothermal ageing at high temperature and presence of organoclay are not additive in the nylon 6 matrix.

(c) The greatest morphological changes caused by hygrothermal ageing at 70 °C were found in the outermost layers of the injection moulded bars. This led to stiffening of the skin region, hence accentuating the skin/core structure.

(d) When nylon or its nanocomposites are exposed to ambient humidity, moisture is rapidly adsorbed onto the surface. This is evident from the *low* indentation modulus results determined at depths of ~1 μm on dried samples compared to the *high* modulus values obtained from the "bulk" tensile tests.

Acknowledgements

We wish to thank the CRC for Advanced Composite Structures and the Australian Research Council for continuing financial support of this project on "*Polymer Nanocomposites*".

References

[1] Jia N, Fraenkel HA, Kagan VA. Effects of moisture conditioning methods on mechanical properties of injection molded nylon 6. J Reinf Plast Compos 2004;23(7):729–37.
[2] Mohd Ishak ZA, Berry JP. Hygrothermal aging studies of short carbon fiber reinforced nylon 6.6. J Appl Polym Sci 1994;51(13):2145–55.
[3] Bergeret A, Pires I, Foulc MP, Abadie B, Ferry L, Crespy A. The hygrothermal behaviour of glass-fibre-reinforced thermoplastic composites: a prediction of the composite lifetime. Polym Test 2001;20(7):753–63.
[4] Usuki A, Koiwai A, Kojima Y, Kawasumi M, Okada A, Kurauchi T, et al. Interaction of nylon 6-clay surface and mechanical properties of nylon 6-clay hybrid. J Appl Polym Sci 1995;55(1):119–23.
[5] Liu L, Qi Z, Zhu X. Studies on nylon 6/clay nanocomposites by melt-intercalation process. J Appl Polym Sci 1999;71(7):1133–8.
[6] Lan T, Pinnavaia TJ. Clay-reinforced epoxy nanocomposites. Chem Mater 1994;6(12):2216–9.
[7] Chow WS, Teoh JK, Lim LY. Mechanical and hygrothermal aging study on polystyrene/organo-montmorillonite nanocomposites. Polym Plast Technol Eng 2008;47(10):1040–5.
[8] Chow WS, Bakar AA, Mohd IZA. Water absorption and hygrothermal aging study on organo-montmorillonite reinforced polyamide 6/polypropylene nanocomposites. J Appl Polym Sci 2005;98(2):780–90.
[9] Killgore JP, Jensen T, Peila R, Sangari SS, Seferis JC. Assessment of durability in high performance polymeric and polynanomeric matrix composites. In: International SAMPE technical conference – materials and processing: sailing into the future; 2004. p. 407–16.
[10] Jana S, Zhong WH. FTIR study of ageing epoxy resin reinforced by reactive graphitic nano-fibers. J Appl Polym Sci 2007;106(5):3555–63.
[11] Vlasveld DPN, Groenewold J, Bersee HEN, Picken SJ. Moisture absorption in polyamide-6 silicate nanocomposites and its influence on the mechanical properties. Polymer 2005;46(26):12567–76.
[12] Vlasveld DPN, Groenewold J, Bersee HEN, Mendes E, Picken SJ. Analysis of the modulus of polyamide-6 silicate nanocomposites using moisture controlled variation of the matrix properties. Polymer 2005;46(16):6102–13.
[13] Lonnroth N, Muhlstein CL, Carlo Pantano, Yue Y. Nanoindentation of glass wool fibers. J Non-Cryst Solids 2008;354(32):3887–95.
[14] Tay CJ, Quan C, Gopal M, Shen L, Akkipeddi R. Nanoindentation techniques in the measurement of mechanical properties of InP-based free-standing MEMS structures. J Micromech Microeng 2008;18(2):025015–24.
[15] Xie S, Zhang S, Liu H, Chen G, Feng M, Qin H. Effects of processing history and annealing on polymorphic structure of nylon-6/montmorillonite nanocomposites. Polymer 2005;46(14):5417–27.
[16] Yalcin B, Valladares D, Cakmak M. Amplification effect of platelet type nanoparticles on the orientation behavior of injection molded nylon 6 composites. Polymer 2003;44(22):6913–25.
[17] Liu TX, Tjiu WC, He CB, Na SS, Chung T-S. A processing-induced clay dispersion and its effect on the structure and properties of polyamide 6. Polym Int 2004;53(4):392–9.
[18] Yu Z-Z, Yang MB, Zhang QX, Zhao CG, Mai Y-W. Dispersion and distribution of organically modified montmorillonite in nylon-66 matrix. J Polym Sci Part B: Polym Phys 2003;41(11):1234–43.
[19] Khanna YP, Kuhn WP. Measurement of crystalline index in nylons by DSC: complexities and recommendations. J Polym Sci Part B: Polym Phys 1997;35(14):2219–31.
[20] Bell TJ, Bendeli A, Field JS, Swain MV, Thwaite EG. The determination of surface plastic and elastic properties by ultra micro-indentation. Metrologia 1991;28(6):463–9.
[21] Oliver WC, Pharr GM. An improved technique for determining hardness and elastic modulus using load and displacement sensing indentation experiments. J Mater Res 1992;7(6):1564–8.
[22] Ngan AHW, Tang B. Viscoelastic effects during unloading in depth-sensing indentation. J Mater Res 2002;17(10):2604–10.
[23] Chavarria F, Shah RK, Hunter DL, Paul DR. Effect of melt processing conditions on the morphology and properties of nylon 6 nanocomposites. Polym Eng Sci 2007;4(11):1847–64.
[24] Kim SW, Jo WH, Lee MS, Ko MB, Jho JY. Effects of shear on melt exfoliation of clay in preparation of nylon 6/organoclay nanocomposites. Polym J 2002;34(3):103–11.
[25] Dennis HR, Hunter DL, Chang D, Kim S, White JL, Cho JW, et al. Effect of melt processing conditions on the extent of exfoliation in organoclay-based nanocomposites. Polymer 2001;42(23):9513–22.
[26] Chow WS, Ishak ZAM, Karger-Kocsis J. Morphological and rheological properties of polyamide 6/poly(propylene)/organoclay nanocomposites. Macromol Mater Eng 2005;290(2):122–7.
[27] Murthy NS, Curran SA, Aharoni SM, Minor H. Premelting crystalline relaxations and phase transitions in nylon 6 and 6,6. Macromolecules 1991;24(11):3215–20.
[28] Roldan LG, Rahl F, Paterson AR. Investigation of polymer order by X-ray diffraction. J Polym Sci – Part C: Polym Symposia 1965;1(8):145–58.
[29] Li T-C, Ma J, Wang M, Tjiu WC, Liu TX, Huang W. Effect of clay addition on the morphology and thermal behaviour of polyamide 6. J Appl Polym Sci 2007;103(2):1191–9.
[30] Fornes TD, Paul DR. Crystallization behavior of nylon 6 nanocomposites. Polymer 2003;44(14):3945–61.
[31] Hiramatsu N, Hirakawa S. Melting and transformation behavior of gamma form nylon 6 under high pressure. Polym J 1982;14(3):165.
[32] Liu XH, Wu QJ. Phase transition in nylon 6/clay nanocomposites on annealing. Polymer 2002;43(6):1933–6.
[33] Kojima Y, Usuki A, Kawasumi M, Okada A, Kurauchi T, Kamigaito O, et al. Novel preferred orientation in injection-molded nylon 6-clay hybrid. J Polym Sci Part B: Polym Phys 1995;33(7):1039–45.
[34] Miyasaka K, Isomoto T, Koganeya H, Uehara K, Ishikawa K. Nylon-6 alpha - phase crystal: chain repeat distance and modulus in the chain direction at low temperature. J Polym Sci Part A-2: Polym Phys 1980;18(5):1047–52.
[35] Tashiro K, Tadokoro H. Calculation of three-dimensional elastic constants of polymer crystals. III. α and γ forms of nylon 6. Macromolecules 1981;14(3):781–5.
[36] Shen L, Phang IY, Liu TX. Nanoindentation studies on polymorphism of nylon 6. Polym Test 2006;25(2):249–53.
[37] Deng X, Chawla N, Chawla KK, Koopman M, Chu JP. Mechanical behaviour of multilayered nanoscale metal-ceramic composites. Adv Eng Mater 2005;7(12):1099–108.
[38] Shen L, Phang IY, Chen L, Liu TX, Zeng K. Nanoindentation and morphological studies on nylon 66 nanocomposites. I. Effect of clay loading. Polymer 2004;45(10):3341–9.
[39] Shen L, Tjiu WC, Liu TX. Nanoindentation and morphological studies on injection-molded nylon-6 nanocomposites. Polymer 2005;46(25):11969–77.
[40] Dasari A, Yu Z-Z, Mai Y-W. Nanoscratching of nylon 66-based ternary nanocomposites. Acta Mater 2007;55(2):635–46.
[41] Fornes TD, Paul DR. Modeling properties of nylon 6/clay nanocomposites using composite theories. Polymer 2003;44(17):4993–5013.
[42] Shen YL, Guo YL. Indentation modelling of heterogeneous materials. Modell Simul Mater Sci Eng 2001;9(5):391–8.